Journal of Photochemistry & Photobiology A: Chemistry 384 (2019) 112029

Contents lists available at ScienceDirect

Journal of Photochemistry & Photobiology A: Chemistry

journal homepage: www.elsevier.com/locate/jphotochem

Difference of photodegradation characteristics between single and mixed VOC pollutants under simulated sunlight irradiation

Zhuang Wang[a,b], Xiaofeng Xie[b,*], Xiao Wang[b], Asad Mahmood[b], Hanxun Qiu[a], Jing Sun[b,*]

[a] University of Shanghai for Science and Technology, 516 Jungong Road, Shanghai, 200093, China
[b] Shanghai Institute of Ceramics, Chinese Academy of Sciences, 1295 Dingxi Road, Shanghai 200050, China

ARTICLE INFO

Keywords:
Photocatalysis
rGO@TiO_2
VOC mixture removal
P-xylene
Benzene derivatives

ABSTRACT

In realistic Volatile organic compounds (VOC)-containing polluted air, VOCs often do not exist alone, but different VOCs coexist. The interaction between different VOCs affects their photodegradation. However, few studies have focused on the photodegradation of mixed VOCs. Herein, rGO-TiO_2 photocatalysts were synthesized by a modified refluxing-solvothermal method, and applied to photocatalytic degradation of single VOC (p-xylene and ethylene) and VOC mixture (containing benzene, toluene, p-xylene). It was found that rGO-TiO_2 possessed higher photocatalytic degradation activity for single VOC and VOC mixture than pure TiO_2. The increased single VOC adsorption capacity, more efficient light harvesting ability, and enhanced separation efficiency of electron-hole were responsible for improved degradation performance of rGO-TiO_2. In addition, superoxide radicals played a more important role than hydroxyl radicals for removing both p-xylene and ethylene. Interestingly, commercial TiO_2 (P25) underwent decreased efficiency (80.0% to 63.8%) in photodegrading from single p-xylene to p-xylene in VOC mixture, while it was remained unchanged (93.5%–93.0%) for T0.2G (0.2% mass ratio of reduced graphene oxide to TiO_2). This could be mainly attributed to sufficient adsorption sites provided by rGO sheets to mitigate competitive adsorption. Simultaneously, its photocatalytic activity showed no obvious decrease after five photodegradation cycles of mixed VOCs. These results suggested great potential of efficient photodegradation of VOC mixture by rGO-TiO_2.

1. Introduction

Volatile organic compounds (VOCs) are a major group of indoor air pollutants, including various alcohols, aromatics (benzene, toluene, xylene), aldehydes, and halocarbons. VOCs, which are released from household products, have proven to be harmful to human health [1,2]. Several techniques have been developed to remove them, such as adsorption [3,4], thermal catalysis [5,6], ozone oxidation [7], photocatalytic oxidation [8]. Photocatalytic oxidation, a green advanced oxidation technology with low energy consumption and strong oxidizing ability, has attracted increasing attentions in the degradation of pollutants. TiO_2-based photocatalyst [9–15] was the most widely used in the field of photocatalysis because of its low cost, high stability, non-toxicity and high reactivity, etc.

Recently, carbon materials, as a cocatalyst, are widely studied, owing to excellent optical and electrical properties. Reduced graphene oxide (rGO), a two-dimensional carbon material, possesses superior in-plane electron transport capability, large specific surface area, and abundant surface π bonds, which are beneficial to improve electron-hole separation efficiency and adsorption capacity of target pollutant molecules. So far, there have been a lot of researches about the photodegradation of aqueous pollutants (methylene blue [16–18], Rhodamine B [19–22], methyl orange [23,24], acetaminophen [25], 5-fluorouracil [26], bisphenol A [27], phenol [28], Cr^{6+} [29]) by rGO-TiO_2 composites. Their photocatalytic degradation activities were promoted after adding optimal amount of rGO. It is suggested that rGO, as a cocatalyst, shows great potential in promoting photodegradation of gaseous pollutants. Hemarj M et al. [30] synthesized anatase TiO_2-graphene oxide (GO) nanocomposites with different GO loadings and evaluated their photocatalytic activity by the degradation of gaseous benzene under UV light irradiation. They found that the existence of GO enhanced photocatalytic degradation activity and attributed it to the improved separation of photogenerated electron-hole pairs. Jungho Ryu et al. [31] developed new hybrid geometry of TiO_2 and reduced-graphene oxides and tested its gaseous acetaldehyde oxidation. The self-assembled composite showed advantages compared to other types of graphene-TiO_2, such as the stronger electronic coupling between rGO sheets and TiO_2, minimized light-shielding effect by rGO. Lin et al. [32]

* Corresponding authors.
E-mail addresses: xxfshcn@163.com (X. Xie), jingsun@mail.sic.ac.cn (J. Sun).

https://doi.org/10.1016/j.jphotochem.2019.112029
Received 13 May 2019; Received in revised form 5 August 2019; Accepted 7 August 2019
Available online 08 August 2019

explored the adsorption and degradation of gaseous acetaldehyde and o-xylene using rGO-TiO_2 photocatalysts. The higher adsorption capacity of o-xylene was observed under the same condition. They also revealed the different roles of active species in the degradation of acetaldehyde and o-xylene. Although many previous works about rGO-TiO_2 for VOCs removal were reported, there are a great variety of VOCs and their properties are different. The mechanism of photodegradation of VOCs by rGO-TiO_2 needs to be explored. In reality, VOCs often do not exist as single specie in polluted air, but several kinds coexist. The interaction between different VOCs affects their photodegradation, thus, it is necessary to investigate photocatalytic degradation of VOC mixture by rGO-TiO_2.

Herein, rGO-TiO_2 composites were synthesized through a modified refluxing-solvothermal method. The light harvesting, electron-hole separation, VOCs adsorption of as-synthesized samples were characterized. The photodegradation mechanism of two typical single VOC (p-xylene and ethylene) were analyzed, and the potential application for the degradation of VOC mixture (containing benzene, toluene and p-xylene) was also investigated. The rGO-TiO_2 composites showed an enhanced photodegradation towards both p-xylene and ethylene than pure TiO_2. The improved VOC mixture degradation performance and cyclic stability further indicate the potential for practical applications.

2. Experimental

2.1. Chemicals and materials

Tetrabutyl titanate (TBOT) and hydrochloric acid (HCl) were purchased from Sinopharm Chemical Reagent CO., Ltd. Absolute ethanol was supplied by Shanghai Zhenxing CO., Ltd. Deionized (DI) water was produced by a Milli-Q system (R > 18.1 MΩ). Graphene oxide (SE2430W) was purchased from The Sixth Element (Changzhou) Materials Technology CO., Ltd. P-benzoquinone (PBQ) and 2,2,6,6-tetramethyl-1-piperidinyloxy (TEMPO) were purchased from Aladdin Industrial Corporation. All chemicals used in our study were of analytical grade and used without further purification.

2.2. Photocatalysts synthesis

The few layers graphene oxide (GO) used in the experiment was obtained by multiple centrifugation of commercial multilayer graphene oxide. Briefly, 1 g of commercial multilayer graphene oxide was added into 500 ml H_2O. Then the suspension was centrifuged at 8000 rpm for several times, with obvious precipitate at the bottom of centrifuge tube removed every time. The obtained GO aqueous suspension (1 mg/mL) was stored at room temperature and used for further experiments. The preparation of composite samples of graphene oxide and titanium dioxide was based on the previous report [32]. Briefly, 5.0 g of TBOT was added into a round bottom flask containing 400 mL absolute ethanol. Then 4 mL deionized water was dropwise added into the solution, followed by refluxing under magnetic stirring at 100 °C for 6 h. The as-prepared amorphous TiO_2 was washed first with absolute ethanol and then deionized water. After that, amorphous TiO_2 were dispersed into the mixture of 50 mL H_2O and 25 mL absolute ethanol, of which the pH was adjusted to 4 by adding a few drops of hydrochloric acid. An appropriate amount of GO aqueous suspension was dropped into it. The suspension was stirred for 6 h and ultrasonicated further for 1 h. Then it was transferred to a Teflon-lined stainless-steel autoclave (Volume 100 mL) and kept at 180 °C for 4 h. The precipitate was washed with absolute ethanol and deionized water and dried at 60 °C to obtain rGO-TiO_2 photocatalysts. The products were denoted as TxG, where x represents the mass percent ratio of GO to TiO_2. Pure TiO_2 (T0G) was prepared by the same solvothermal treatment without the addition of GO. Degussa P25, commercial titanium dioxide, was also used for comparison.

2.3. Characterization

The morphologies and structures of photocatalysts were characterized by transmission electron microscope (TEM, FEI Electron Optics, Tecnai G2 F20). The X-ray diffraction (XRD) pattern were collected using high resolution powder X-ray diffractometer (BRUKER AXS GMBH, D8 ADVANCE) with Cu Ka radiation (λ = 0.15418 nm, 2θ varied from 20° to 80°, 8°/min). Raman spectra were collected by a DXR Raman Microscope using a laser with an excitation wavelength of 532 nm at laser power of 7 mW (Thermal Scientific Corporation, USA). X-ray photoelectron spectroscopy (XPS) experiments were conducted on a RBD upgraded PHI-5000C ESCA system (Perkin Elmer) with MgKα radiation (1253.6 eV). Fourier transform infrared (FTIR) spectra were measured by a Thermal Scientific 5225 Verona Rd with the KBr pellet technique. UV–vis diffuse reflectance spectra were obtained on a Shimadzu UV-3600 spectrometer by using $BaSO_4$ as reference. Photoluminescence (PL) spectra of the photocatalysts were examined at room temperature by an Edinburgh Instruments FLSP-920 fluorescence spectrophotometer with an excitation wavelength of 320 nm. Photocurrent response measurement of the as-synthesized photocatalysts was conducted using a CHI 660D electrochemical workstation with a conventional three-electrode quartz cell. Before the measurement, the suspension containing 50 mg sample and 2 ml absolute ethanol was coated on FTO glass (1.0 * 2.5 cm) by spin coating for three times, then it was measured as working electrode. Platinum plate and Ag/AgCl electrode were used as counter electrode and reference electrode, respectively. 1 mol/L NaCl was used as an electrolyte solution. An AM1.5 G solar power system was used as light irradiation source. In order to obtain a stable initial photocurrent, firstly it was tested without light irradiation until the photocurrent is stable. Then turn on the light for 10 s, turn off for 10 s for 4 cycles. The photocurrent-time curves were measured at 0.2 V versus Ag/AgCl. Electron spin resonance (ESR) signals of reactive species spin-trapped by 5,5-dimethyl-L-pyrroline-N-oxide (DMPO) were collected on a JES-FA200 spectrometer. Photocatalyst (5 mg) was added into DMPO/ethanol (30 μL/2 mL) solution and DMPO/H_2O (30 μL/2 mL) solution for detecting superoxide radicals ($\cdot O_2^-$) and hydroxyl radicals (·OH), respectively. Then the solution will be irradiated for 5 min. under a 500 W Xenon lamp before starting measurement.

2.4. Dark absorption and photocatalytic degradation measurements

Both of dark absorption and photocatalytic degradation were carried out in a flowing-mode gas phase photocatalytic online test system same with the previous report [32], which consisted of a gas mixer, a reaction chamber and gas chromatograph. First, 0.1 g photocatalyst was coated on glass plate with 15*7.5 cm size. Then the glass plate was placed into a reaction chamber and sealed with a quartz glass, with flowing VOCs passed through. The concentration of single p-xylene is 25 ppm with the flow rate as 80 ml/min and that of ethylene is 250 ppm with the flow rate as 8 ml/min. In VOC mixture, the concentration of all three gaseous pollutants is 10 ppm with the flow rate as 80 ml/min. First, the gaseous pollutant is introduced into the reaction chamber under dark condition, which is called as the dark adsorption process. When the dark adsorption reaches adsorption-desorption equilibrium, the Xenon lamp will be turned on and photocatalytic degradation will begin at the same time. The distance of samples and light resource was kept at 30 cm for all experiments. The 250 W and 500 W Xenon lamp were used as light resource. The concentration of p-xylene or ethylene in the reaction chamber was monitored by gas chromatography (equipped with a flame ionization detector and methane reforming furnace) in real time. The degradation efficiency of p-xylene or ethylene was calculated by using the formula: $(1 - C/C_0) \times 100\%$, where C_0 is the initial concentration and C is the concentration of p-xylene or ethylene at different time intervals. Cyclic stability measurement was to carry out photocatalytic degradation measurement for 5 times on the

same sample. The time interval between two cycles was 10 days. The sample of cyclic stability measurement was just placed at ambient temperature and pressure for next cycle.

2.5. TPD measurements

Temperature-programmed desorption (TPD) measurements of photocatalysts were conducted using ChemiSorb PCA-1200 (Builer, China). Briefly, 0.1 g photocatalyst was placed into electric furnace and heated at 393 K for 1 h with flowing high-purity N_2. When the temperature dropped to room temperature, the pollutant valve was opened and VOC was passed through the quartz tube at a flowing rate of 40 ml/min for 2 h. Then, the pollutant valve was closed, and the TCD signal of desorbed pollutant gas was monitored by increasing the temperature from room temperature to 800 °C at a heating rate of 10 °C per minute in N_2.

2.6. Scavenger experiments

The operation of scavenger experiments was basically the same as the photocatalytic degradation process. The difference between the two experiments lies in that the scavenger experiment needs to add corresponding active species scavenger (2,2,6,6-tetramethylpiperidine oxide, TEMPO, ·OH scavenger and p-benzoquinone, PBQ, $\cdot O_2^-$ scavenger). During the test, 0.01 g TEMPO or PBQ was mixed with 0.1 g photocatalyst, then the mixture was coated onto a glass plate for scavenger experiments. As a reference, sample without any scavenger was also tested.

3. Results and discussions

3.1. Characterization of photocatalysts

Fig. 1 shows the TEM images of as-synthesized graphene oxide, TiO_2 and T0.2 G. Graphene oxide with pleated sheet structure is observed (Fig. 1a). Titanium dioxide particles, with a size around 10 nm (Fig. 1b), are supported on graphene sheets (Fig. 1c–d). Further, the interface of TiO_2 and graphene oxide is shown by high resolution TEM, which indicates that there is a certain interface coupling between graphene oxide and TiO_2. Besides, the lattice fringe spacing of 0.35 nm corresponds to the (101) crystal plane of anatase TiO_2 (Fig. 1d).

X-ray diffraction (XRD) was conducted to investigate the crystal structures of pure TiO_2 and graphene oxide composite samples as shown in Fig. 2a. The typical peaks at 25.1°, 37.8°, 47.9° and 54.4° indicate that TiO_2 nanocrystals in all samples are crystallized in anatase phase (JCPDS No. 21-1272). The rGO-TiO_2 nanocomposites with different weight ratios of rGO exhibit a similar XRD pattern of anatase TiO_2, indicating that compounding rGO with TiO_2 has no effect on its phase structure. Moreover, there is no significant peak shift observed, meaning that no doping occurred. Raman spectroscopy measurements was also carried out to characterize crystal structure of these samples. Fig. 2b displays the Raman spectra of TiO_2 and rGO-TiO_2 samples. The typical peaks at 144 cm^{-1}, 394 cm^{-1}, 514 cm^{-1} and 636 cm^{-1} correspond to anatase phase [33], consistent with the XRD results. In the Raman spectra of rGO- TiO_2, another two peaks (1350 cm^{-1} and 1600 cm^{-1}) are observed, which is ascribed to the reduced graphene oxide [34]. They are characteristic D band and G band of reduced graphene oxide. In addition, as shown in the enlarged Raman spectra, the peak at 144 cm^{-1} (Eg) is shifted to the higher wave number (Fig. 2c). Because the Eg peak is mainly attributed to the symmetric stretching vibration of O—Ti—O of TiO_2, this means that there exists interfacial interaction between the TiO_2 and the rGO. The O1s of XPS spectra is shown in Fig. S1, it is seen that the bind energy of surface O shifts from 531.51 (T0G) to 531.62 eV (T0.2G), indicating the chemical bond could be formed between the TiO_2 and the rGO, which is consistent with Raman spectra. The Raman spectra of D band and G band before and after solvothermal reaction are presented in the Fig. 2d. D band around 1350 cm^{-1} represents the presence of sp^3 disordered carbon and defects, whereas G band 1600 cm^{-1} represents the in-plane vibration of ordered sp^2 carbon atoms [35]. By comparison, the intensity ratio of the D band and the G band is increased after solvothermal treatment, which is due to the removal of oxygen functional groups and subsequently leads to a decrease of ordered sp^2 carbon atoms and/or increase of sp^3 disordered carbon and defects. The intensity of G band of T0.2G is smaller than that of GO, meaning that the in-plane C network is re-established [36]. And it has been reported that reduction of GO would induce the increase of I_D/I_G ratio [18,24,25,27]. Therefore, these results imply that graphene oxide is reduced.

Table 1 gives the BET specific surface area of the as-prepared materials. Compared with T0G, T0.2G and T0.5G have the slight increased BET specific surface area, and T1G has the basically same value, which

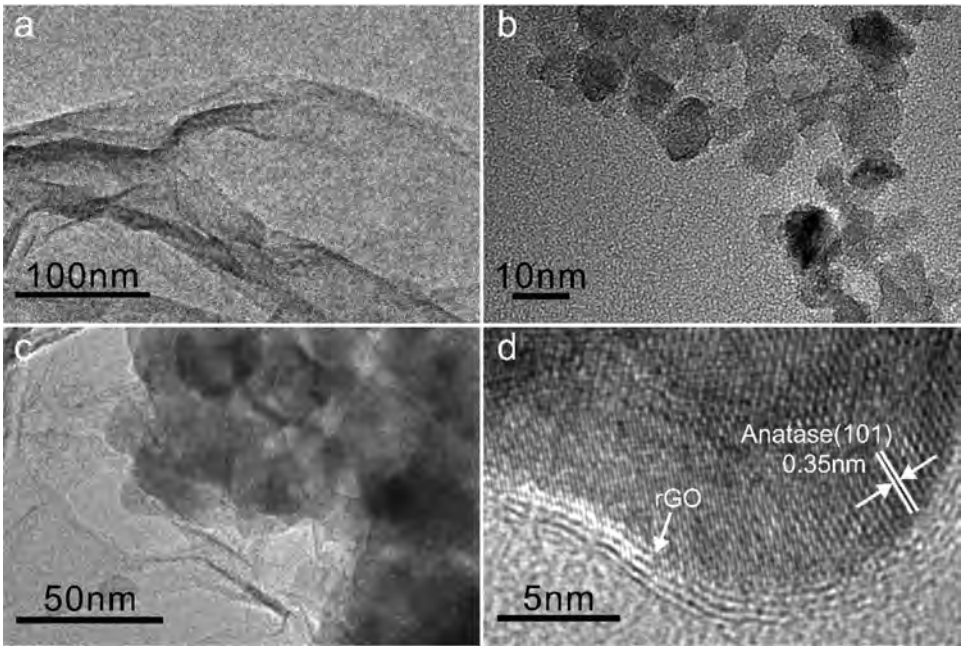

Fig. 1. TEM images of (a) GO, (b) T0G and (c) T0.2 G; HRTEM image of (d) T0.2 G.

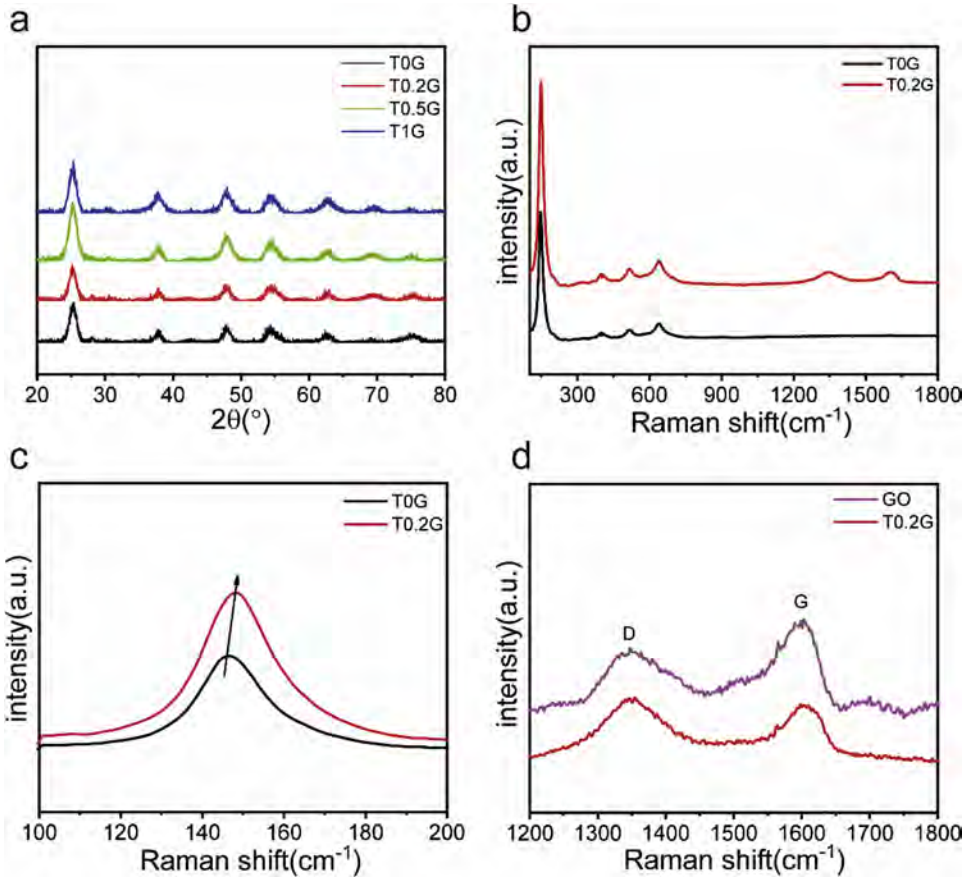

Fig. 2. (a) XRD patterns of T0G and TxG; (b, c, d) Raman spectra of T0G, T0.2 G and GO.

Table 1
BET specific surface area of as-synthesized photocatalysts.

Sample	T0G	T0.2G	T0.5G	T1G
Specific surface area (m^2/g)	174.06	190.72	189.94	174.07

indicates the high content of rGO in composites will not increase specific surface area. The increase in the specific surface area of rGO-TiO_2 could be mainly due to the high specific surface area of GO and improved dispersion of TiO_2 particles.

3.2. Dark absorption of single p-xylene and ethylene

Dark adsorption is an important step that is carried out before photocatalytic degradation, which reflects the ability to adsorb specific gas molecules. As shown in Fig. 3a, it is obvious that there is continuous improvement in the amount of p-xylene adsorption with the increased amount of reduced graphene oxide. In the case of ethylene, we set a very slow flow rate (8 ml/min). The adsorption capacity is obviously increased for the composite samples and shows an increasing trend same with p-xylene. The inset figure of Fig. 3a–b displays histograms of integral value of dark adsorption curves, corresponding to the adsorption capacity of all the samples. By comparison, it can be clearly seen that the adsorption capacity of ethylene is significantly lower than that of p-xylene, which could be attributed to the π-π interaction of graphene and p-xylene. These results suggest that rGO is beneficial to enhance the adsorption of VOCs and tends to adsorb aromatic VOCs.

To further prove enhanced absorption ability, temperature-programmed desorption measurement (TPD) was conducted. Fig. 3c shows that more p-xylene desorbed from the surface of T0.2G, consistent with the results of dark adsorption. Surprisingly, the T0.2G has three peaks in the TPD curve, which might be ascribed to physically adsorbed p-xylene on the surface of the composite for peak 1, chemically absorbed p-xylene on the surface of TiO_2 for peak 2 and π-π interaction of graphene and p-xylene for peak 3. For ethylene, the amount of desorbed ethylene gradually increases with temperature rising, however the desorption signal begins to decrease when the temperature is at about 300 °C shown in Fig. 3d. Compared with the T0G, T0.2G exhibits a larger amount of desorbed ethylene, indicating that the composite can markedly enhance the adsorption of ethylene on the surfaces, especially for the chemically adsorbed form. These results demonstrate the positive effect of reduced graphene oxide on the adsorption of VOCs.

3.3. Photocatalytic degradation of single VOC (p-xylene and ethylene) and VOC mixture (containing benzene, toluene, p-xylene)

The photocatalytic activity of P25, pure TiO_2 and rGO-TiO_2 composites was evaluated by monitoring the concentration change of flowing gaseous p-xylene or ethylene during degradation process. For eliminating the influence of photolysis of gaseous pollutants, the photocatalytic activity of blank sample (without photocatalyst) were also tested. The degradation activity of p-xylene and ethylene is shown in the Figs. 4 and 5. Without photocatalysts, no obvious photolysis of ethylene and p-xylene occurred. The influence of light intensity on the degradation has also been investigated. Under the irradiation of 500 W Xenon light, the degradation efficiency of p-xylene for the samples with or without graphene ranges between 70% and 80% (Fig. 4a). However, under 250 W Xenon light, the enhanced photodegradation effect of reduced graphene oxide is more prominent (Fig. 4b). The degradation efficiency of T0.2G reaches 43.5% of p-xylene in 90 min. irradiation while P25, T0G, T0.5G and T1G only reaches 11.4%, 26.2%, 37.2% and 31.2%, respectively (Fig. 4c). These results illustrate that photocatalytic

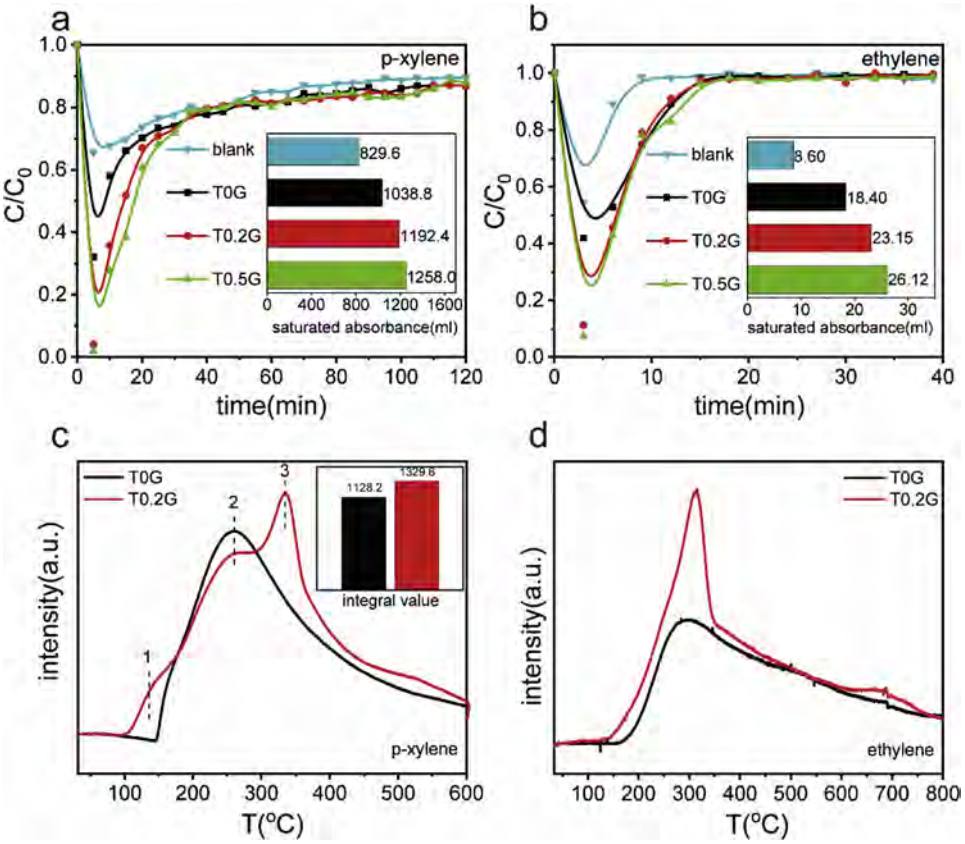

Fig. 3. Adsorption of dynamic gaseous (a) p-xylene and (b) ethylene for different samples in dark condition and corresponding saturated adsorption capacity (inset of (a) and (b)); (c) p-xylene-TPD and ethylene-TPD of T0G and T0.2 G, the inset (c): integrate area of TPD curve.

degradation activity of p-xylene is improved within a certain range and then exhibits a declined trend. In addition, P25 began to deactivate after 10 min of light-on irradiation. In Fig. 5, the degradation efficiency for T0G, T0.2G, and T0.5G reaches 73.8%, 90.2% and 75.3% respectively, in 120 min, having consistent degradation trend with that of p-xylene. And P25 just reaches 50.6% under the same experiment condition. Photodegradation results of ethylene and p-xylene demonstrate that rGO can enhance the photocatalytic activity of pure TiO_2 and the performance of T0.2 G is much better than commercial P25. Moreover, there exists an optimal value for the added amount of graphene oxide. When present in a high content, although reduced graphene oxide can adsorb more gaseous pollutants and promote photogenerated electron-hole pairs separation, it could disadvantageously occupy some active sites of TiO_2 and shield part of the light radiations illuminated to TiO_2, leading to the decreased photocatalytic activity [37,38].

Based on above experimental results, it has been known that the composites are beneficial to improve the photocatalytic degradation activity of two typical VOCs (p-xylene and ethylene). However, there are more than one VOC in the realistic environment, so common gaseous benzene derivatives mixture (containing 10 ppm benzene, 10 ppm toluene and 10 ppm p-xylene) are selected to further study the ability of T0.2G to degrade VOC mixture and evaluate its cyclic stability. As presented in Fig. 6a, T0.2G exhibits an excellent photocatalytic activity (72.2% in 2 h), compared with P25 (27.1% in 2 h). The adsorption difference of benzene derivatives is shown in Fig. 6b. The saturated adsorption amounts of benzene, toluene and p-xylene are 172 ml, 483.2 ml, 937.2 ml, respectively. This indicates that the order of the affinity toward T0.2 G surface is benzene < toluene < p-xylene, which is in agreement with previous reports [39–42]. The difference could be ascribed to the stronger dispersion interaction from the additional methyl groups [40]. In mixed VOCs (Fig. 6c), the degradation efficiencies of benzene, toluene and p-xylene are 30.6%, 85.4% and

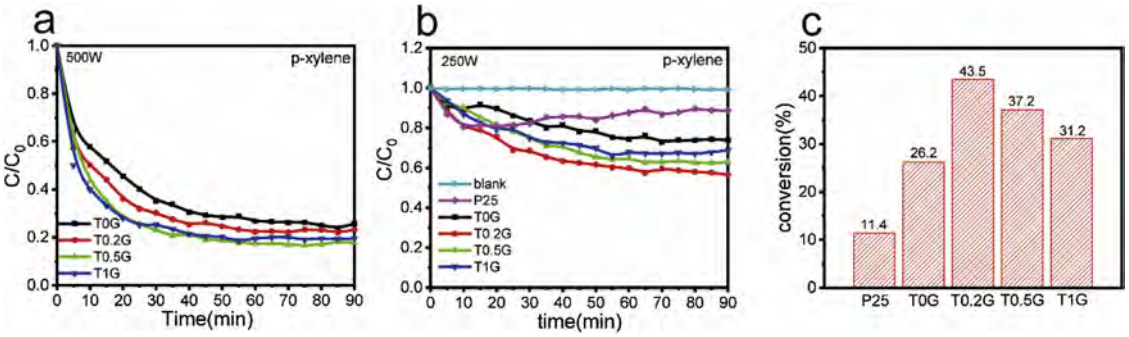

Fig. 4. Photocatalytic degradation of flowing gaseous p-xylene under (a) 500 W and (b) 250 W Xenon lamp irradiation and (c) comparison of degradation efficiency of five different photocatalysts under 250 W Xenon lamp irradiation.

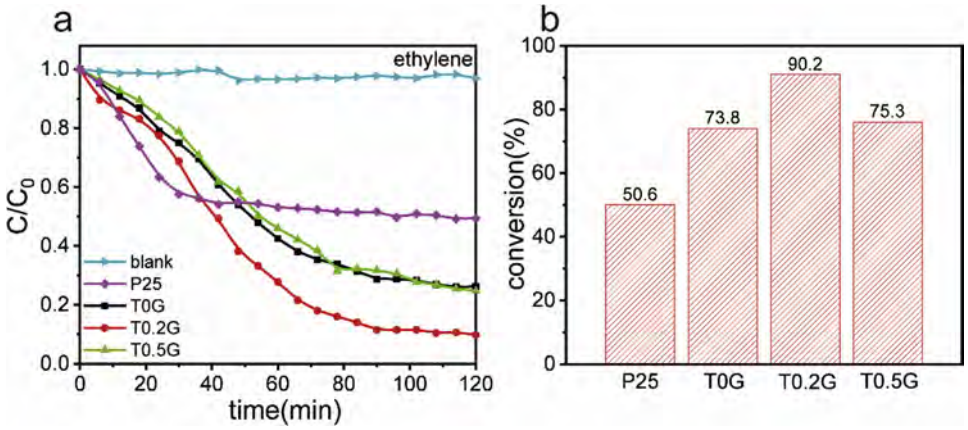

Fig. 5. Photocatalytic degradation of flowing gaseous (a) ethylene and (b) the comparison of degradation efficiency of four different photocatalysts under 500 W Xenon lamp irradiation.

93.0%, respectively. The difference of degradation mainly comes from two aspects: on the one hand, in the process of degrading VOCs, gas adsorption has a great influence on the photocatalytic oxidation of VOCs. Based on above adsorption data, adsorption affinity order toward T0.2G surface is benzene < toluene < p-xylene, consistent with the order of degradation on T0.2 G surface. This indicates that adsorption could be the dominant factor responsible for degradation difference. On the other hand, the different difficulty level of benzene, toluene and p-xylene oxidation might also be responsible for difference of degradation. As we all know, benzene has a more stable aromatic structure with respect to chemical or thermal attack because of higher C–H bond energy [43,44]. As for the oxidation of toluene and xylene, attacks occurred more easily from methyl [45–47], p-xylene with two methyl is relatively easier to be oxidized. In addition, Fig. 6d indicates that T0.2G has improved degradation of three pollutants in mixed gas compared to P25, in which benzene possesses the largest enhancement, then toluene, and finally p-xylene. Comparison of conversion of single p-xylene and p-xylene in mixed gas is shown in Fig. 6e. P25 undergoes decreased efficiency (80.0% to 63.8% in 2 h) in photodegrading from single p-xylene to p-xylene in VOC mixture, while it was remained unchanged (93.5% to 93.0%) for T0.2G. This indicates T0.2G has stronger environmental adaptability, which is important for air purification. Besides, Fig. 6f displays cyclic stability evaluation result, which suggests that T0.2G is able to maintain a relatively high activity after 5 cycles although there might be VOCs adsorbed on the surface [Fig. S2]. Moreover, Fig. S3 shows XRD of T0.2G before and after cyclic stability test. After 5 cycles, there was no significant change in crystal structure, indicating T0.2 G has excellent stability. Therefore, these results imply the great potential of such composite photocatalyst in environment remediation, especially for VOC mixture.

In order to investigate the intrinsic causes of improved photocatalytic degradation of single VOC (p-xylene and ethylene) and VOC mixture (containing benzene, toluene, p-xylene) in composite samples, we further characterized their optical properties, fluorescence emission, photocurrent response.

The UV–vis diffuse reflectance spectra were measured to investigate the optical properties of all the photocatalysts (Fig. 7a). Among them, P25 has the weakest light harvesting ability. Specifically, with reduced

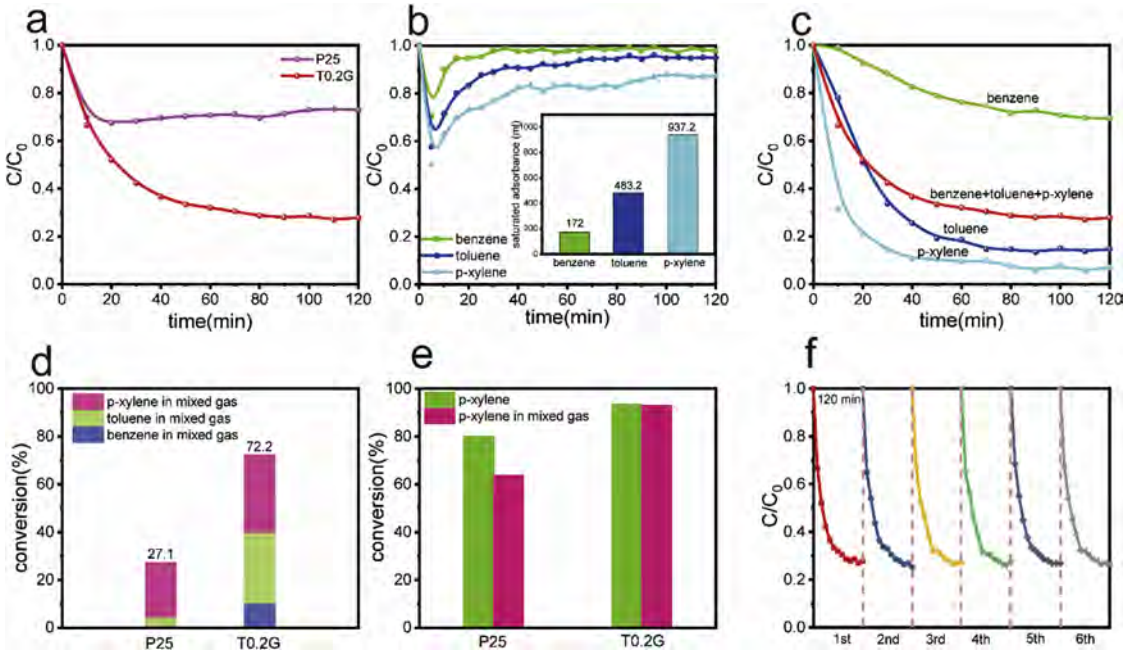

Fig. 6. (a) Photocatalytic degradation curve of flowing mixed gaseous benzene, toluene and p-xylene, (b) dark adsorption and corresponding saturated adsorption capacity (inset of (b)), (c) degradation curve of single gas in mixed gaseous pollutants by T0.2 G, (d) degradation efficiency of commercial P25 and T0.2 G (including efficiency ratio in mixed gas), (e) comparison of conversion of single p-xylene and p-xylene in mixed gas, (f) cyclic stability of T0.2 G.

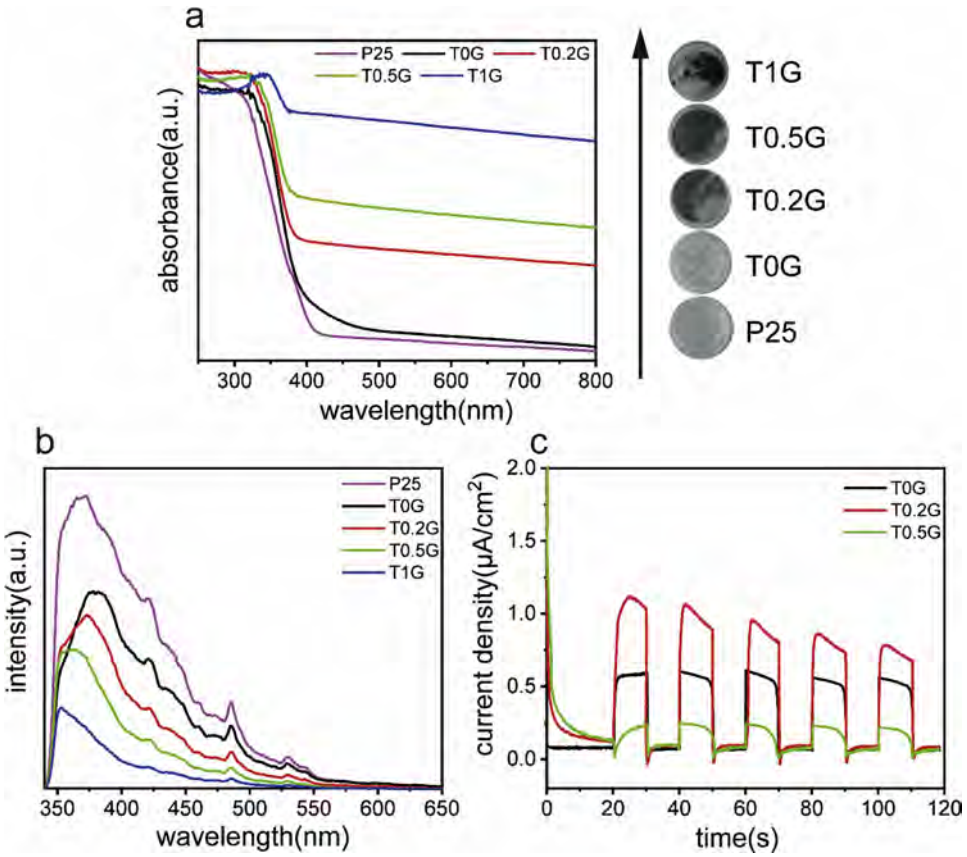

Fig. 7. (a) UV–vis diffuse reflectance spectra and photograph, (b) PL spectra at an excitation wavelength of 320 nm, (c) photocurrent curves of the as-prepared samples.

graphene oxide increasing in the composite, the light absorption of composite samples strengthens and the absorption edge shifts towards longer length, which is ascribed to the formation of chemical bond between TiO_2 and rGO (Figs. 2c, S1), which reduces the bandgap energy of the TiO_2/rGO composite. Such an analogous phenomenon is also observed in previous research studies regarding TiO_2/rGO nanocomposites, which can be attributed to the interfacial interaction between the TiO_2 and the rGO [19,24,25,29,30]. The color change of samples is consistent with these results, which indicate spectral absorption capacity of composites is upgraded by the introduction of reduced graphene oxide and spectral excitation range is broadened. Fig. 7b displays the PL spectra of P25 and the as-prepared photocatalysts. Typically, photoluminescence (PL) analysis is conducted to investigate the migration and separation efficiency of photogenerated electron- hole pairs in a semiconductor, as the PL emission mainly arises from charge-carriers combination [48]. The results show that PL intensity of photocatalysts diminished as reduced graphene oxide in the composite increased, which suggests reduced graphene oxide can effectively inhabit electrons and holes recombination in the composites by electron transfer to reduced graphene oxide [49], which is critical for subsequent generation of active species and surface reactions. In addition, photocurrent response was measured in 10 s light on-off cycles. To exclude the influence of oxidation of rGO, Raman spectra of T0.2G before and after photocurrent measurement was measured (Fig. S4). It is seen that there is no significant change in I_D/I_G. Generally, D band around 1350 cm^{-1} represents the presence of sp3 disordered carbon and defects, and G band 1600 cm^{-1} represents the in-plane vibration of ordered sp2 carbon atoms. Therefore, it is considered to be still reduced graphene oxide (rGO). Fig. 7c displays the photocurrent response of T0G, T0.2G and T0.5G. Obviously, compared with T0G, T0.2G presents higher photocurrent response, which indicates that more electrons are transferred to the photoelectrode and higher separation efficiency of the photogenerated electrons and holes of T0.2G. Because, on the one hand, the Fermi level of rGO is more positive than the conduction band of TiO_2 [50], so that photogenerated electrons tend to move toward the reduced graphene oxide, thereby suppressing photogenerated electron-hole pairs recombination. On the other hand, the high electrical conductivity of rGO enables these electrons to transport in the two-dimensional π-conjugation structures of rGO rather than recombination with holes that remain in the valence band of TiO_2 [51]. Whereas T0.5 G has lower photocurrent response, which could be due to shading effect of too much rGO [37,38].

3.4. Mechanisms of photocatalytic degradation of ethylene and p-xylene

To further explore the mechanism of photocatalytic degradation, we conducted ESR and scavenger experiments to evaluate the ability of composites to produce active species (·OH and $\cdot O_2^-$) and the role of different types of active species in photocatalytic processes. The ESR signals of DMPO-·OH and DMPO-$\cdot O_2^-$ are shown in Fig. 8a–b. It can be clearly informed that the signal intensity of superoxide radicals is significantly greater than the signal intensity of hydroxyl radicals. This indicates that the as-synthesized materials are capable of producing more superoxide radicals under irradiation than hydroxyl radicals. In Fig. 8a, it can be clearly seen that the amount of superoxide radicals decreases with the addition and increased content of rGO. This could be attributed to that photogenerated electrons migrating to the rGO layer through the coupling interface are captured by the defects on the rGO [32], leading to the decrease in the amount of $\cdot O^{2-}$ formed (O_2 + e-→ · O_2-). Whereas Fig. 8b displays that the amount of hydroxyl radicals increases slightly with the addition of rGO and that of T0.2 G and T0.5 G basically remains equal, which could be ascribed to longer

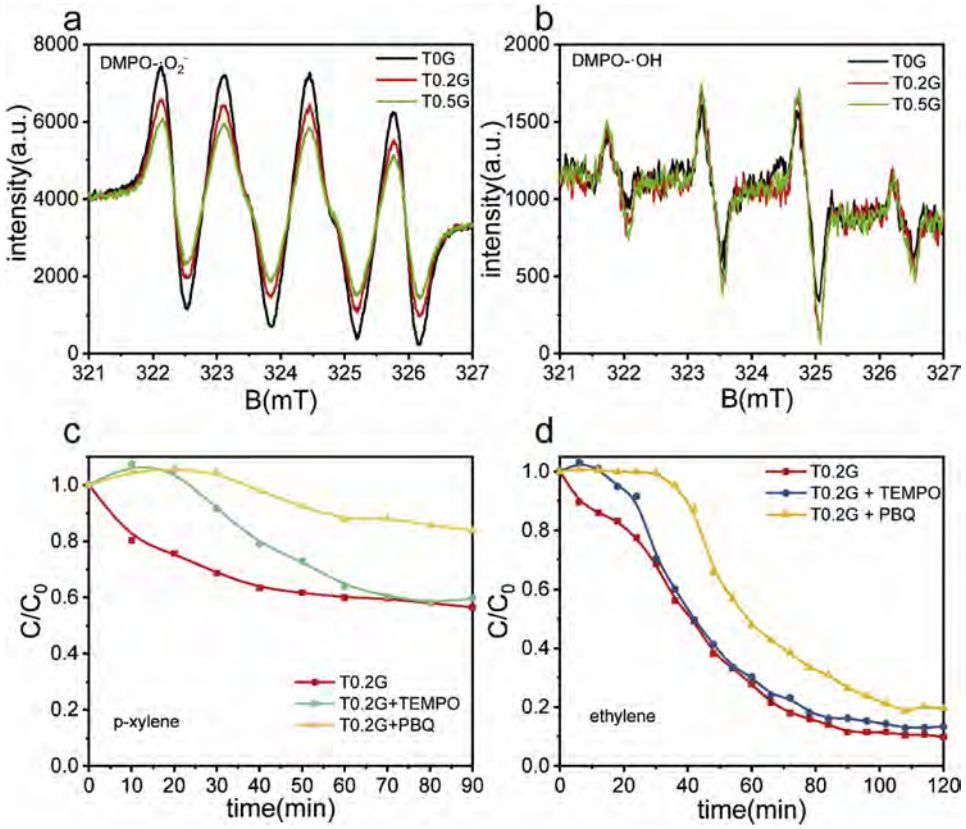

Fig. 8. (a) Superoxide radicals ($\cdot O_2^-$) signal with DMPO as scavenger in ethanol (b) Hydroxyl radicals (·OH) signal with DMPO as scavenger in water; (c, d) Scavenger experiments using PBQ and TEMPO as corresponding $\cdot O_2^-$ and ·OH scavenger.

lifetime of holes because of transfer of photogenerated electrons to rGO ($H_2O + h^+ \rightarrow \cdot OH + H^+$). In addition, we took 0.01 g of 2,2,6,6-tetramethylpiperidine oxide (TEMPO, ·OH scavenger) and p-benzoquinone (PBQ, $\cdot O_2^-$ scavenger), respectively, and incorporated them to 0.1 g of T0.2 G composite and tested photocatalytic degradation activity of ethylene and p-xylene. The results are shown in Fig. 8c–d. As can be informed from the two figures, no matter it is ethylene or p-xylene, the degradation efficiency of T0.2 G whose superoxide radicals are captured declined more than that of T0.2 G whose hydroxyl radicals are captured, indicating that superoxide radicals have a more important role in photocatalytic degradation process of these two VOCs. This result is also well supported by the ESR result.

Based on the above analysis, the possible mechanism of enhanced photocatalytic degradation of p-xylene and ethylene by rGO/TiO_2 could be proposed as follows (Fig. 9). Under Xenon lamp irradiation, Titanium dioxide generates photogenerated electrons and holes. Part of the surface photogenerated electrons transfer to the reduced graphene oxide sheet, which thus inhibit electrons and holes recombination. A portion of the electrons transferred to the reduced graphene oxide sheet are captured by defects on the reduced graphene oxide sheet, and a portion of that react with oxygen and thus form superoxide radicals. The photogenerated electrons of titanium dioxide itself also react with oxygen to produce superoxide radicals [27]. Hydroxyl radicals are generated mainly from the reaction of photogenerated holes with surface hydroxyl and water. In the process of degrading p-xylene, p-xylene adsorbed on the surface of composites is mainly degraded by hydroxyl radicals and superoxide radicals, and superoxide radicals are the main reactive radicals. As shown in Fig. S5, with the photocatalytic degradation of p-xylene, carbon dioxide (up to 160 ppm) is also produced simultaneously. Except for CO_2 and H_2O, Some intermediate products such as terephthalic acid [52], toluene [53], etc. could also be formed during the degradation process. In the process of degrading ethylene, in addition to a similar degradation mechanism to p-xylene, ethylene adsorbed on the surface of titanium dioxide might experience other oxidation pathways (e.g. hole oxidation…) based on the scavenger experiments. Similarly, in this process, it is also possible to form intermediates such as acetaldehyde or acetic acid [54].

4. Conclusion

Binary nanocomposites with interface coupling between reduced graphene oxide and TiO_2 were synthesized via a modified refluxing-solvothermal method. With the addition of rGO, the photocatalytic degradation activity of single p-xylene and ethylene was enhanced. And 0.2% mass ratio (of graphene to TiO_2) had the optimal photocatalytic efficiency. This could be ascribed to larger gas pollutant adsorption capacity, more efficient light harvesting ability, and more importantly, higher electron-hole pairs separation efficiency. In addition, superoxide radicals played a more important role in degrading both p-xylene and ethylene. In the degradation of VOC mixture, the photodegradation of mixed VOCs was improved by 2.6 times compared with commercial P25 and photodegradation efficiency decreased in the order of p-xylene > toluene > benzene. Furthermore, P25 underwent decreased efficiency (80.0% to 63.8% in 2 h) in photodegrading from single p-xylene to p-xylene in mixed VOCs, while it was remained unchanged (93.5% to 93.0%) for T0.2 G. Moreover, it could still remain excellent photocatalytic activity after 5 cycles. Overall, our work explored photodegradation activity and mechanism of different types of single VOC and investigated photodegradation characteristics of mixed VOCs. It is hoped that our work could offer a strong support for in-depth study of rGO-TiO_2 composites with improved photocatalytic activity and stability in environment remediation.

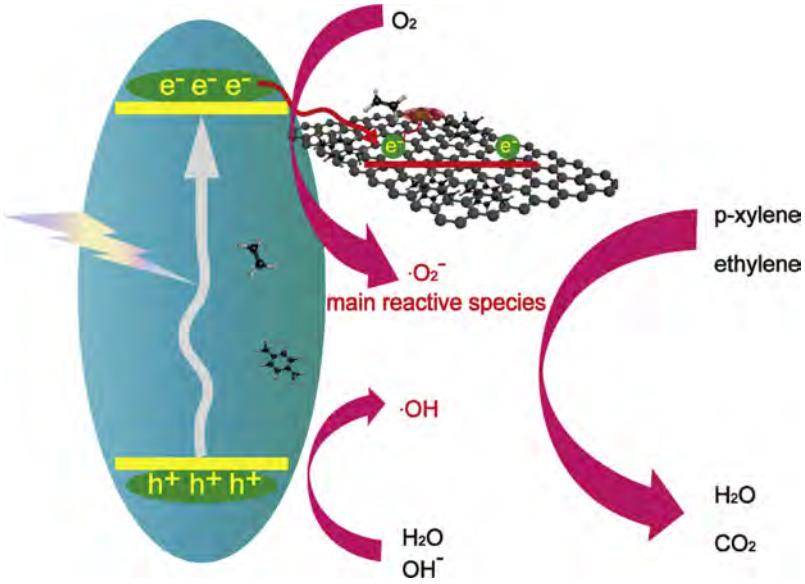

Fig. 9. Schematic diagrams of possible photocatalytic degradation mechanism of p-xylene and ethylene on rGO-TiO_2 nanocomposite.

Declaration of Competing Interest

The authors declare no competing financial interest.

Acknowledgements

This work was financially supported by the National Key Research and Development Program of China (2016YFA0203000), the NSFC-DFG bilateral organization program (51761135107) and Shanghai Sailing Program (18YF1426800).

Appendix A. Supplementary data

Supplementary material related to this article can be found, in the online version, at doi:https://doi.org/10.1016/j.jphotochem.2019.112029.

References

[1] J. Li, X. Liu, Z. Sun, L. Pan, Novel Bi2MoO6/TiO2 heterostructure microspheres for degradation of benzene series compound under visible light irradiation, J. Colloid Interface Sci. 463 (2016) 145–153.
[2] E. Marco-Urrea, X. Gabarrell, G. Caminal, T. Vicent, C.A. Reddy, Aerobic degradation by white-rot fungi of trichloroethylene (TCE) and mixtures of TCE and perchloroethylene (PCE), J. Chem. Technol. Biotechnol. 83 (2008) 1190–1196.
[3] T.K. Poddar, K.K. Sirkar, A hybrid of vapor permeation and membrane-based absorption-stripping for VOC removal and recovery from gaseous emissions, J. Memb. Sci. 132 (1997) 229–233.
[4] E. Dumont, G. Darracq, A. Couvert, C. Couriol, A. Amrane, D. Thomas, Y. Andres, P. Le Cloirec, VOC absorption in a countercurrent packed-bed column using water/silicone oil mixtures: influence of silicone oil volume fraction, Chem. Eng. J. 168 (2011) 241–248.
[5] H. Wang, W. Yang, P. Tian, J. Zhou, R. Tang, S. Wu, A highly active and anti-coking Pd-Pt/SiO2 catalyst for catalytic combustion of toluene at low temperature, Appl. Catal. A-Gen. 529 (2017) 60–67.
[6] M. Piumetti, D. Fino, N. Russo, Mesoporous manganese oxides prepared by solution combustion synthesis as catalysts for the total oxidation of VOCs, Appl. Catal. B-Environ. 163 (2015) 277–287.
[7] H. Xiao, R. Liu, X. Zhao, J. Qu, Enhanced degradation of 2,4-dinitrotoluene by ozonation in the presence of manganese(II) and oxalic acid, J. Mol. Catal. A-Chem. 286 (2008) 149–155.
[8] V. Hequet, C. Raillard, O. Debono, F. Thevenet, N. Locoge, L. Le Coq, Photocatalytic oxidation of VOCs at ppb level using a closed-loop reactor: the mixture effect, Appl. Catal. B-Environ. 226 (2018) 473–486.
[9] R. Asahi, T. Morikawa, T. Ohwaki, K. Aoki, Y. Taga, Visible-light photocatalysis in nitrogen-doped titanium oxides, Science 293 (2001) 269–271.
[10] H.G. Yang, C.H. Sun, S.Z. Qiao, J. Zou, G. Liu, S.C. Smith, H.M. Cheng, G.Q. Lu, Anatase TiO2 single crystals with a large percentage of reactive facets, Nature 453 (2008) 638-U634.
[11] S.U.M. Khan, M. Al-Shahry, W.B. Ingler, Efficient photochemical water splitting by a chemically modified n-TiO2, Science 297 (2002) 2243–2245.
[12] J. Zhang, J.H. Bang, C. Tang, P.V. Kamat, Tailored TiO2-SrTiO3 heterostructure nanotube arrays for improved photoelectrochemical performance, ACS Nano 4 (2010) 387–395.
[13] X.Z. Li, F.B. Li, Study of Au/Au3+-TiO2 photocatalysts toward visible photooxidation for water and wastewater treatment, Environ. Sci. Technol. 35 (2001) 2381–2387.
[14] X. Pan, M.-Q. Yang, X. Fu, N. Zhang, Y.-J. Xu, Defective TiO2 with oxygen vacancies: synthesis, properties and photocatalytic applications, Nanoscale 5 (2013) 3601–3614.
[15] X. Chen, L. Liu, P.Y. Yu, S.S. Mao, Increasing solar absorption for photocatalysis with black hydrogenated titanium dioxide nanocrystals, Science 331 (2011) 746–750.
[16] J. Hu, H. Li, Q. Wu, Y. Zhao, Q. Jiao, Synthesis of TiO2 nanowire/reduced graphene oxide nanocomposites and their photocatalytic performances, Chem. Eng. J. 263 (2015) 144–150.
[17] J. Hu, H. Li, S. Muhammad, Q. Wu, Y. Zhao, Q. Jiao, Surfactant-assisted hydrothermal synthesis of TiO2/reduced graphene oxide nanocomposites and their photocatalytic performances, J. Solid State Chem. 253 (2017) 113–120.
[18] N. Sun, J. Ma, C. Wang, J. Xue, L. Qiang, J. Tang, A facile and efficient method to directly synthesize TiO2/rGO with enhanced photocatalytic performance, Superlatt. Microstruct. 121 (2018) 1–8.
[19] D. Liang, C. Cui, H. Hu, Y. Wang, S. Xu, B. Ying, P. Li, B. Lu, H. Shen, One-step hydrothermal synthesis of anatase TiO2/reduced graphene oxide nanocomposites with enhanced photocatalytic activity, J. Alloys Compd. 582 (2014) 236–240.
[20] Q. Chen, M. Zhou, Z. Zhang, T. Tang, T. Wang, Preparation of TiO2 nanotubes/reduced graphene oxide binary nanocomposites enhanced photocatalytic properties, J. Mater. Sci.-Mater. Electron. 28 (2017) 9416–9422.
[21] H. Xing, W. Wen, J.-M. Wu, One-pot low-temperature synthesis of TiO2 nanowire/rGO composites with enhanced photocatalytic activity, RSC Adv. 6 (2016) 94092–94097.
[22] Q. Tong, Y.-M. Dong, L. Yan, D.-N. He, High-efficient synthesis and photocatalytic properties of Ag/AgBr/TiO2 monolithic photocatalysts using sodium alginate as substrate, J. Inorg. Mater. 32 (2017) 637–642.
[23] M. Nasr, S. Balme, C. Eid, R. Habchi, P. Miele, M. Bechelany, Enhanced visible-light photocatalytic performance of electrospun rGO/TiO2 composite nanofibers, J. Phys. Chem. C 121 (2017) 261–269.
[24] Z. Lu, G. Chen, W. Hao, G. Sun, Z. Li, Mechanism of UV-assisted TiO2/reduced graphene oxide composites with variable photodegradation of methyl orange, RSC Adv. 5 (2015) 72916–72922.
[25] A.H.C. Khavar, G. Moussavi, A.R. Mahjoub, The preparation of TiO2@rGO nanocomposite efficiently activated with UVA/LED and H2O2 for high rate oxidation of acetaminophen: catalyst characterization and acetaminophen degradation and mineralization, Appl. Surf. Sci. 440 (2018) 963–973.
[26] S.V. Nipane, S.-W. Lee, G.S. Gokavi, A.N. Kadam, In situ one pot synthesis of nanoscale TiO2-anchored reduced graphene oxide (RGO) for improved photodegradation of 5-fluorouracil drug, J. Mater. Sci.-Mater. Electron. 29 (2018) 16553–16564.
[27] L. Xu, L. Yang, E.M.J. Johansson, Y. Wang, P. Jin, Photocatalytic activity and mechanism of bisphenol a removal over TiO2-x/rGO nanocomposite driven by visible light, Chem. Eng. J. 350 (2018) 1043–1055.
[28] N.S. Alim, H.O. Lintang, L. Yuliati, Iop, photocatalytic removal of phenol over titanium dioxide-reduced graphene oxide photocatalyst, 10th Joint Conference on Chemistry, (2016).

[29] L. Liu, C. Luo, J. Xiong, Z. Yang, Y. Zhang, Y. Cai, H. Gu, Reduced graphene oxide (rGO) decorated TiO2 microspheres for visible-light photocatalytic reduction of Cr (VI), J. Alloys Compd. 690 (2017) 771–776.
[30] H.M. Yadav, J.-S. Kim, Solvothermal synthesis of anatase TiO2-graphene oxide nanocomposites and their photocatalytic performance, J. Alloys Compd. 688 (2016) 123–129.
[31] J. Ryu, S. Kim, H.I. Kim, E.-H. Jo, Y.K. Kim, M. Kim, H.D. Jang, Self-assembled TiO2 agglomerates hybridized with reduced-graphene oxide: a high-performance hybrid photocatalyst for solar energy conversion, Chem. Eng. J. 262 (2015) 409–416.
[32] W. Lin, X. Xie, X. Wang, Y. Wang, D. Segets, J. Sun, Efficient adsorption and sustainable degradation of gaseous acetaldehyde and o-xylene using rGO-TiO2 photocatalyst, Chem. Eng. J. 349 (2018) 708–718.
[33] P. Song, X. Zhang, M. Sun, X. Cui, Y. Lin, Graphene oxide modified TiO2 nanotube arrays: enhanced visible light photoelectrochemical properties, Nanoscale 4 (2012) 1800–1804.
[34] Y. Zhang, N. Zhang, Z.-R. Tang, Y.-J. Xu, Improving the photocatalytic performance of graphene-TiO2 nanocomposites via a combined strategy of decreasing defects of graphene and increasing interfacial contact, J. Chem. Soc. Faraday Trans. 14 (2012) 9167–9175.
[35] D. Graf, F. Molitor, K. Ensslin, C. Stampfer, A. Jungen, C. Hierold, L. Wirtz, Spatially resolved raman spectroscopy of single- and few-layer graphene, Nano Lett. 7 (2007) 238–242.
[36] G. Rajender, P.K. Giri, Formation mechanism of graphene quantum dots and their edge state conversion probed by photoluminescence and Raman spectroscopy, J. Mater. Chem. C 4 (2016) 10852–10865.
[37] H. Fakhri, A.R. Mahjoub, H. Aghayan, Effective removal of methylene blue and cerium by a novel pair set of heteropoly acids based functionalized graphene oxide: adsorption and photocatalytic study, Chem. Eng. Res. Des. 120 (2017) 303–315.
[38] G. Zhang, Y. Sun, C. Zhang, Z. Yu, Decomposition of acetaminophen in water by a gas phase dielectric barrier discharge plasma combined with TiO2-rGO nanocomposite: mechanism and degradation pathway, J. Hazard. Mater. 323 (2017) 719–729.
[39] P.M. Staehelin, A. Valerio, S.M.D.A. Guelli Ulson de Souza, A. da Silva, J.A. Borges Valle, A.A. Ulson de Souza, Benzene and toluene removal from synthetic automotive gasoline by mono and bicomponent adsorption process, Fuel 231 (2018) 45–52.
[40] N. Klomkliang, D.D. Do, D. Nicholson, Affinity and packing of benzene, toluene, and p-Xylene adsorption on a graphitic surface and in pores, Ind. Eng. Chem. Res. 51 (2012) 5320–5329.
[41] D. Farmanzadeh, A. Valipour, Adsorption of benzene and toluene molecules on surface of pure and doped cadmium oxide nanosheets: a computational investigation, Appl. Surf. Sci. 450 (2018) 509–515.
[42] O. Borck, E. Schroder, Methylbenzenes on graphene, Surf. Sci. 664 (2017) 162–167.
[43] G.E. Davico, V.M. Bierbaum, C.H. Depuy, G.B. Ellison, R.R. Squires, The C-H bond-Energy of benzene, J. Am. Chem. Soc. 117 (1995) 2590–2599.
[44] J. Chen, X. Chen, X. Chen, W. Xu, Z. Xu, H. Jia, J. Chen, Homogeneous introduction of CeOy into MnOx-based catalyst for oxidation of aromatic VOCs, Appl. Catal. B-Environ. 224 (2018) 825–835.
[45] Y. Huang, S.S.H. Ho, Y. Lu, R. Niu, L. Xu, J. Cao, S. Lee, Removal of indoor volatile organic compounds via photocatalytic oxidation: a short review and prospect, Molecules 21 (2016).
[46] C.C. Pei, W.W.-F. Leung, Photocatalytic oxidation of nitrogen monoxide and o-xylene by TiO2/ZnO/Bi2O3 nanofibers: optimization, kinetic modeling and mechanisms, Appl. Catal. B-Environ. 174 (2015) 515–525.
[47] M. Sleiman, P. Conchon, C. Ferronato, J.-M. Chovelon, Photocatalytic oxidation of toluene at indoor air levels (ppbv): towards a better assessment of conversion, reaction intermediates and mineralization, Appl. Catal. B-Environ. 86 (2009) 159–165.
[48] Z. Lu, L. Zeng, W. Song, Z. Qin, D. Zeng, C. Xie, In situ synthesis of C-TiO2/g-C3N4 heterojunction nanocomposite as highly visible light active photocatalyst originated from effective interfacial charge transfer, Appl. Catal. B-Environ. 202 (2017) 489–499.
[49] J. Liu, Z. Wang, L. Liu, W. Chen, Reduced graphene oxide as capturer of dyes and electrons during photocatalysis: surface wrapping and capture promoted efficiency, J. Chem. Soc. Faraday Trans. 13 (2011) 13216–13221.
[50] Y.-J. Yu, Y. Zhao, S. Ryu, L.E. Brus, K.S. Kim, P. Kim, Tuning the graphene work function by electric field effect, Nano Lett. 9 (2009) 3430–3434.
[51] N.J. Bell, N. Yun Hau, A. Du, H. Coster, S.C. Smith, R. Amal, Understanding the enhancement in photoelectrochemical properties of photocatalytically prepared TiO2-reduced graphene oxide composite, J. Phys. Chem. C 115 (2011) 6004–6009.
[52] E. Perez, J. Fraga-Dubreuil, E. Garcia-Verdugo, P.A. Hamley, W.B. Thomas, D. Housley, W. Partenheimer, M. Poliakoff, Selective aerobic oxidation of para-xylene in sub- and supercritical water. Part 1. Comparison with ortho-xylene and the role of the catalyst, Green Chem. 13 (2011) 2389–2396.
[53] I. Dhada, M. Sharma, P.K. Nagar, Quantification and human health risk assessment of by-products of photo catalytic oxidation of ethylbenzene, xylene and toluene in indoor air of analytical laboratories, J. Hazard. Mater. 316 (2016) 1–10.
[54] B. Hauchecorne, T. Tytgat, S.W. Verbruggen, D. Hauchecorne, D. Terrens, M. Smits, K. Vinken, S. Lenaerts, Photocatalytic degradation of ethylene: an FTIR in situ study under atmospheric conditions, Appl. Catal. B-Environ. 105 (2011) 111–116.